PHYSICAL REVIEW B VOLUME 20, NUMBER 12 15 DECEMBER 1979

Self-image excitation mechanism for fast ions scattered by metal surfaces at grazing incidence

A. A. Lucas*
IBM Thomas J. Watson Research Center, Yorktown Heights, New York 10598
(Received 10 July 1979)

Energy-loss spectra and electronic-transition probabilities of atomic and molecular ions scattered by surface plasmons are evaluated for experiments in which fast ions are specularly reflected from a metal surface at grazing incidence. The coupling between plasmons and the ion monopole charge governs the scattered-ion loss spectrum. For ion velocities not small compared to plasmon phase velocities and for small grazing angles, large numbers of surface plasmons may be excited, resulting in large average energy losses and broad loss spectra, as observed experimentally. Further, the interaction between the ion multipole moments with the surface plasmons induces transitions between ground and excited states of the ions. For molecular ions this may result in their dissociation when the state produced is unstable. The final electronic states populated by the plasmon scattering mechanism are shown to exhibit a high degree of orientation, as required by the observation of elliptically polarized fluorescence emitted by the scattered beam. As applications, we calculate explicitly the dissociative scattering of H_2^+ and the production of coherently oriented $2P$ states in He^+ and compare with available experimental results.

I. INTRODUCTION

Processes of charge and energy exchanges between fast ions and solid surfaces are of considerable current interest in several branches of physics. As reviewed in a recent book,[1] advances have been made in identifying the numerous ion-solid interactions responsible for the richness of the observed phenomena.

In relatively recent works, the production of excited atomic or molecular states of the projectile particles has been investigated both in reflection at surfaces[2] and in transmission through foils.[3] The electronic excitation process may manifest itself through the dissociation of the excited, unstable molecular ion[2] and/or through the fluorescence of the scattered beam.[4-7]

In the interpretation of the results of these experiments on metal targets, the role played by the image fields of the ions in the surface has been alluded to without, however, receiving a detailed quantitative treatment. It is the purpose of the present paper to contribute to the investigation of the image effects in situations where they are likely to be important, namely in cases of grazing-incidence scattering.

As expected from the concept of channeling and confirmed experimentally, e.g., by Andrä *et al.*,[6,7] fast ions with kinetic energies from a few keV to a few hundred keV, incident upon a smooth surface at grazing angles less than a few degrees, do not penetrate into the target but are subjected to a predominantly specular scattering by the first surface layer of target atoms. This fact results in the effective elimination of a number of complex phenomena associated with ion penetration such as sputtering, multiple bulk scattering, secondary emission, electron stripping, etc. In such favorable circumstances, it is possible to analyze the inelastic scattering at the surface in terms of a reduced Hamiltonian which includes only the long-range coupling of the ion multipole operators to the surface plasmon field outside of the metal target. The short-range, elastic part of the surface atom potential is assumed to provide a specular, elastic trajectory for the ion position coordinates which enter the ion-plasmon Hamiltonian as time-dependent parameters.[8]

The dominant processes are then as follows: The permanent monopole and fluctuating higher multipoles of the scattered ion produce excitations of the surface plasmon field at the expense of its forward kinetic energy. The excited surface plasmons are, in turn, able to excite dipolar and higher-multipolar transitions in the scattered ions.[9] In this way, the metal surface mediates a coupling between otherwise independent multipoles of the ions and induces conversion of kinetic energy into electronic excitation energy in both the projectile and target.

A description of the above processes in terms of scattering of the ion static image charge by the ion dipole moment, although illuminating from the physical point of view, would be quantitatively incorrect, as we shall see, because of the dynamical nature of the metal response to the ion-charge distribution at fast ion velocities (i.e., $v_{\text{ion}} \gtrsim v_F$, the Fermi velocity).

This paper is organized as follows: First, we introduce and justify our working Hamiltonian (Sec. II). Then we analyze the energy spectrum of unexcited scattered ions as induced by loss processes to the surface plasmons (Sec. III). Dipole-raising transitions are investigated in Sec. IV. Finally,

in Sec. V, we apply the theory to several practical cases. For H_2^+ scattering we find that dissociation by excitation of the $2p\sigma_u$ unstable state is very likely for all ion kinetic energies down to a few hundred eV. For $He^+(1S \rightarrow 2P)$ transitions and similar transitions in other ions, we evaluate the production of coherent atomic $2P$ states and obtain the degree of elliptical polarization of the light emitted by subsequent radiative decay of the scattered beam. The paper concludes with some possible further extensions and applications of the model-collective Hamiltonian.

II. MODEL HAMILTONIAN

The geometry of the scattering problem and the coordinate notations used are shown in Fig. 1. We have two "particles" separately coupled to one boson field.

One particle is the incoming ion monopole with free Hamiltonian

$$H_m = \frac{P^2}{2M} + V_s(\vec{R}), \tag{1}$$

where P and M are the ion momentum and mass, and where $V_s(\vec{R})$ is the short-range surface potential of the first atomic layer of the metal surface. We will make no assumption regarding V_s other than it provides for elastic specular reflection at some parameter distance Z_0 of closest approach to the surface. For this to be realistic, the incidence angle Φ of the beam with the surface must be smaller than the critical angle Φ_c for surface channeling, that is such that the ion interacts with the surface by a sequence of correlated, small-angle forward scatterings resulting in specular reflection.[10] In model calculations, Φ_c typically varies from 10° to 2° for protons of kinetic energy from a few hundred eV to a few hundred keV on Al(110).[10] Experiments[7] with 300 keV Ar^+ ions on a Cu surface confirm that for $\Phi < 5°$, a well-defined forward-scattered peak around 2Φ is observed and unambiguously attributed to Ar^+ ions specularly reflected. In addition to this surface-channeling argument, our assumption of specular scattering may be operationally justified by the possibility of setting the spectrometer position and aperture to effectively discard the diffuse part of the scattered beam.

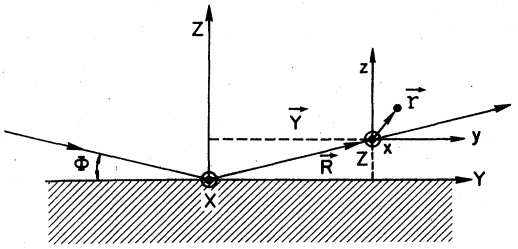

FIG. 1. Coordinate systems used to describe the ion-specular trajectory $\vec{R}(t)$ and the electron position operator $\vec{r}$.

The second particle is the "active" electron on the ion, i.e., the actual electron of H_2^+ or He^+, etc., or the effective electron of heavier ions taking part in the raising transition of interest. Its free Hamiltonian is

$$H_e = \frac{p^2}{2m} + V_{\text{ion}}(\vec{r}) \tag{2}$$

and has the discrete plus continuum spectrum of the ion. $\vec{r}$ is the electron-dipole operator connecting the initial and final states under consideration.

The boson field is the ensemble of surface plasmons of wave vector $\vec{k}$ parallel to the surface, frequency $\omega_k \simeq \omega_s = \omega_p/\sqrt{2}$, and free Hamiltonian ($\hbar = 1$)

$$H_p = A \int d\vec{k}\, \omega_k (a_k^\dagger a_k + \tfrac{1}{2}), \tag{3}$$

where a_k destroys a plasmon quantum and A is some normalization area of the surface.

The coupling terms between ion, electron, and plasmons have been derived and used earlier in different contexts,[8,12] but for completeness we shall obtain them here from a simple plausibility argument. Owing to its translational invariance for displacements parallel to the continuous surface, the monopole-surface interaction $H_{mp}(\vec{R})$ may be Fourier analyzed as (see Fig. 1 for the coordinate notations)

$$H_{mp} = A \int d\vec{k}\, V_k(Z) e^{i\vec{k}\cdot\vec{Y}}, \quad V_k(Z) = V_{-k}^*(Z). \tag{4}$$

Because H_{mp} must satisfy Laplace's equation, $\Delta_R H_{mp}(\vec{R}) = 0$, and remain everywhere finite, the Fourier coefficients are easily shown to have the form

$$V_k(Z) = \alpha_k e^{-k|Z|}, \quad \alpha_k = \alpha_{-k}^*. \tag{5}$$

The integration constant α_k is the classical amplitude of the $\vec{k}$-surface plasmon. Quantization is achieved by replacing α_k by the manifestly Hermitian operator

$$\alpha_k = C_k(a_k + a_{-k}^\dagger), \tag{6}$$

where C_k is a real constant and where the lowering and raising operators satisfy the quantization rules $[a_k, a_l^\dagger] = (1/A)\delta(\vec{k} - \vec{l})$, etc. The ion-plasmon interaction now is (assuming Z remains positive)

$$H_{mp}(\vec{R}) = A \int d\vec{k}\, C_k e^{-kZ}(a_k e^{i\vec{k}\cdot\vec{Y}} + a_k^\dagger e^{-i\vec{k}\cdot\vec{Y}}). \tag{7}$$

The coupling strength C_k is determined by requir-

ing that, for fixed $\vec{R}$, the plasmon Hamiltonian $H_p + H_{mp}$ contains, in its mean ground state, the classical image-potential energy.[11,13] This yields

$$C_k = \left(\frac{z^2 e^2 \omega_p^2}{8\pi A k \omega_k}\right)^{1/2} S(k), \tag{8}$$

where z is the monopole charge and where $S(k)$ is some cutoff function which removes the divergence of the classical image-potential $z^2e^2/4Z$ when $Z \to 0$. Explicit forms of $S(k)$ will be discussed later (Sec. III).

From (7) the electron-plasmon coupling Hamiltonian is readily obtained in the dipole approximation to which we will restrict ourselves here:

$$H_{ep} = \vec{r} \cdot \frac{\partial}{\partial \vec{R}} H_{mp}(\vec{R}) = A \int d\vec{k} C_k e^{-kZ} (a_k \vec{K} e^{i\vec{k}\cdot\vec{\Upsilon}} + a_k^\dagger \vec{K}^* e^{-i\vec{k}\cdot\vec{\Upsilon}}) \cdot \vec{r}, \tag{9}$$

where

$$\vec{K} = (i\vec{k}, -k). \tag{10}$$

With He^+ in mind, we shall now restrict the electron Hamiltonian to a two-level model consisting of the $1S$ ground state $|0\rangle$, energy E and the triply degenerate $2P$ states, energy E_1, designated here as $|i\rangle$ $(i = x, y, z)$ where the quantization axes are shown in Fig. 1. If c_0 and c_i are electron destruction operators in the corresponding orbitals, the total Hamiltonian will then be, collecting relevant terms,

$$H = \sum_{i=0}^{z} E_i c_i^\dagger c_i + A \int d\vec{k}\, \omega_k a_k^\dagger a_k + A \int d\vec{k} (\gamma_k a_k + \gamma_k^* a_k^\dagger) + A \int d\vec{k} \sum_{i=x,y,z} (\lambda_{ki} a_k + \lambda_{ki}^* a_k^\dagger)(c_0^\dagger c_i + c_i^\dagger c_0), \tag{11}$$

where

$$\gamma_k = C_k e^{-kZ + i\vec{k}\cdot\vec{\Upsilon}}, \tag{12}$$

$$\lambda_{kx,y} = Q_{x,y} C_k i k_{x,y} e^{-kZ + i\vec{k}\cdot\vec{\Upsilon}}, \tag{13}$$

$$\lambda_{kz} = -Q_z C_k k e^{-kZ + i\vec{k}\cdot\vec{\Upsilon}}, \tag{14}$$

and where

$$Q_i = \langle 0 | i | i \rangle \quad (i = x, y, z), \tag{15}$$

are the "dipole lengths" for the corresponding transitions. For the H_2^+ scattering problem, the quantization axis for the electron states will be the molecular axis $\vec{D}$, and suitable modifications of the above Hamiltonian will be introduced in Sec. V.

The monopole Hamiltonian (1) has been discarded, since, for calculating the plasmon response, the ion kinetic energy may be taken as a constant of motion as it, in fact, nearly is. This amounts to treating the $\vec{R}$ variable in (11)–(14) as the time-dependent c number

$$\vec{R} = (\vec{v}_\parallel t, Z_0 + v_\perp |t|), \tag{16}$$

where the origin of time is taken to be the time of specular reflection at Z_0, and where $\vec{v}_\parallel$ and $v_\perp$ are the components of the ion velocity parallel and normal to the surface, respectively. We remark here that Eq. (16) is the simplest trajectory, but it is perhaps not the most appropriate to use for quantitative purposes. Indeed, the strength of the inelastic processes to be discussed depends not only on $\vec{v}_\parallel$ and $v_\perp$, but also on the detailed shape of the ion flight path close to the surface where the interactions are strongest. For instance, a two-parameter hyperbolic path

$$\vec{R}(t) = [\vec{v}_\parallel t, (v_\perp^2 t^2 + Z_1^2)^{1/2} - Z_2] \tag{17}$$

is much closer to the actual trajectory[10] and, as will be seen in Sec. V, yields enhanced effects due to the longer dwelling time in the interaction zone.

Equation (11) will be our working model Hamiltonian. Retaining surface plasmons as the only target excitations with which the beam couples neglects a number of processes besides those which we have already mentioned in the Introduction. The main ones are short-range inelastic scattering phenomena occurring when, and if, the ion penetrates the tail of electron density at the target surface, and processes of charge pick-up (neutralization) and pick-off (ionization). The former will be conveniently ignored, in hopes that for sufficiently small grazing incidence they can be neglected as compared to long-range electronic losses associated with exciting surface plasmons. The latter may be neglected as a first-order process if the forward ion kinetic energy satisfies

$$\tfrac{1}{2} M v_\parallel^2 \gtrsim (I - \Phi_e)\frac{M}{m}, \tag{18}$$

where I is the ion ground-state neutralization energy (i.e., the first ionization potential of the neutral species) and Φ_e is the metal work function. This Einstein-type condition forbids direct neutralization when metal electrons tunneling from the Fermi level must acquire a final kinetic energy superior to the available neutralization energy $I - \Phi_e$. Typically, $\frac{1}{2} M v_\parallel^2 \gtrsim 20$ keV for H_2^+. If $v_\parallel$ is lower than the critical velocity indicated by condition (18), charge neutralization becomes a dominant process and the resulting neutrals can presumably be discriminated against, experimentally, by electrostatic or magnetic deflections and/or by suitable energy analysis.[2] An extension of the

present theory to take charge-transfer process explicitly into account is possible and will be discussed elsewhere.

III. THE LOSS SPECTRUM OF THE PRIMARY IONS

In this section we need to recall, for further use in later sections, some basic results of the study of charge d-particle scattering by surface plasmons. Let us momentarily assume that the incident ions have no internal electronic structure, so that Hamiltonian (11) reduces to

$$H_{\rm red} = A\int d\vec{k}\,\omega_k a_k^\dagger a_k + A\int d\vec{k}\,[\gamma_k(t)a_k + \gamma_k^*(t)a_k^\dagger]\,. \tag{19}$$

This exactly soluble model has been studied by many authors,[8,11-15] mostly in the context of electron spectroscopy. If $|\{0_k\}\rangle$ designates the initial plasmon\ground state, the exact state at time t is

$$|\Psi_0(t)\rangle = e^{-iH_p t}\mathfrak{D}|\{0_k\}\rangle = e^{-iH_p t}|\{I_k^*\}\rangle\,, \tag{20}$$

where

$$\mathfrak{D} = \exp\left\{A\int d\vec{k}\,[I_k^*(t)a_k^\dagger - I_k(t)a_k]\right\} \tag{21}$$

is the plasmon-displacement operator which stretches each plasmon half-field a_k by the coherent amplitude I_k^* according to

$$\mathfrak{D}^\dagger a_k \mathfrak{D} = a_k + I_k^*(t)\,, \tag{22}$$

and where the amplitude is

$$I_k = i\int_{-\infty}^{t} d\tau\,\gamma_k(\tau)e^{-i\omega_k\tau}\,. \tag{23}$$

The meaning of the Glauber state[16] (20) is that when, at time $t=\infty$, an energy measurement is performed on the plasmon system (i.e., in practice, when the scattered-ion energy spectrum is measured, which is equivalent, since overall energy is conserved), the probability of finding $\{n_k\}$ excitations in the final state is a Poisson distribution

$$P(\{n_k\}) = \exp\left(-A\int d\vec{k}\,|I_k|^2\right)\prod_k \frac{|I_k(\infty)|^{2n_k}}{n_k!}\,. \tag{24}$$

The ion energy-loss spectrum which witnesses this distribution can be written in a compact form: The probability for the ion to lose energy ω is the Fourier transform

$$P_0(\omega) = \frac{1}{2\pi}\int_{-\infty}^{+\infty} dt\,e^{i\omega t}P_0(t) \equiv \langle\{I_k^*\}|(H_p - \omega - i\epsilon)^{-1}|\{I_k^*\}\rangle \tag{25}$$

of the correlation function

$$P_0(t) = \langle\{0_k\}|\mathfrak{D}^\dagger e^{-iH_p t}\mathfrak{D}|\{0_k\}\rangle = P_0(0)\exp\left(A\int d\vec{k}\,|I_k|^2 e^{-i\omega_k t}\right). \tag{26}$$

From Green's function theory, (25) is just the density of states at energy ω to be found in the final coherent state $|\{I_k^*\}\rangle$.

Introducing the specular trajectory (16) into the amplitude (23), one obtains the result

$$I_k(t) = -iC_k e^{-kz_0}\left[\frac{\exp(-kv_\perp|t| - i\Omega_k t)}{i\Omega_k + kv_\perp|t|/t} - \left(1+\frac{|t|}{t}\right)\mathrm{Re}(kv_\perp - i\Omega_k)^{-1}\right], \tag{27}$$

where

$$\Omega_k = \omega_k - \vec{k}\cdot\vec{v}_\parallel \tag{28}$$

is a Doppler-shifted plasmon frequency. We shall need this result later, but, for the purpose of this section, we need only consider the asymptotic limit

$$I_k(\infty) = 2iC_k e^{-kz_0}\,\mathrm{Re}\frac{1}{kv_\perp - i\Omega_k} \tag{29}$$

calculated for grazing incidence, i.e., when $v_\perp \to 0$. One finds

$$|I_k|^2 = 4C_k^2 e^{-2kz_0}\frac{kv_\perp}{\Omega_k^2 + k^2v_\perp^2}\,\mathrm{Im}\frac{1}{\Omega_k - ikv_\perp}\,. \tag{30}$$

In calculating the $\vec{k}$ integral in (26) we can make use of

$$\lim_{v_\perp\to 0}\mathrm{Im}\frac{1}{\Omega_k - ikv_\perp} = \pi\delta(\Omega_k) \tag{31}$$

which expresses the resonant excitation of surface plasmons whose phase velocity coincides with the forward ion velocity $\vec{v}_\parallel$. This makes the angular integral trivial:

$$\int_0^{2\pi} d\phi\,\delta(\omega_k - kv_\parallel\cos\phi) = \frac{2}{\omega_k(x^2-1)^{1/2}}\Theta(x-1)\,, \qquad x = kv_\parallel/\omega_s \tag{32}$$

from which the strength of the Poisson distribution in (26) is obtained as

$$Q = A\int d\vec{k}\,|I_k|^2 = \frac{2z^2e^2}{v_\perp}I\,, \tag{33}$$

where

$$I = \int_1^\infty dx\frac{S^2(x)}{x(x^2-1)^{1/2}}e^{-\alpha x}, \quad \alpha = \frac{2\omega_s z_0}{v_\parallel}\,. \tag{34}$$

Note that, according to calculations of Ref. 10, the Z_0 parameter is generally much smaller than 1 Å so that we can put $\alpha = 0$ and ignore the exponential function in the integrand, or incorporate this factor into the cutoff function $S(x)$.

Several cutoff functions $S(x)$ will now be discussed. We have the choice between a sharp step, a smooth exponential, or an algebraic function:

$$S^2(x)=\Theta(x_c-x),\quad S^2(x)=e^{-2x/x_c},$$
$$S^2(x)=[(1+x^2/x_c^2)^{1/2}-x/x_c]^2 \tag{35}$$

$$x_c=k_c v_{\parallel}/\omega_s, \tag{36}$$

where k_c is a parameter of order 1 Å^{-1}. The third form in (35) is obtained from a Thomas-Fermi treatment of the metal surface response to external charges.[17,18] The second form merely amounts to shift the effective image plane inwards of the surface by an amount of order k_c^{-1},[19] a standard procedure to eliminate the classical image-potential divergence. The first form in (35) is appropriate only for large $x_c \gg 1$ and yields the maximum value of the strength Q:

$$Q \leq \frac{\pi z^2 e^2}{v_{\perp}} \quad (x_c \gg 1). \tag{37}$$

For x_c not large compared to 1, one of the two smooth cutoffs must be used. For the purpose of numerical evaluations, we shall be using the exponential form which yields

$$I=\int_{\delta}^{\infty} dz \int_1^{\infty} dx\,(x^2-1)^{-1/2}e^{-zx}=\int_{\delta}^{\infty} dz\,K_0(z), \tag{38}$$

where $K_0(z)$ is a modified Bessel function[20] and where

$$\delta=\frac{2}{x_c}+\alpha=\frac{2\omega_s}{v_{\parallel}}(k_c^{-1}+Z_0). \tag{39}$$

Both K_0 and its integral in (38) are tabulated in Ref. 30. For $v_{\parallel}$ sufficiently small, one can use the approximate form

$$Q=\frac{2z^2e^2}{v_{\perp}}(\pi/2\delta)^{1/2}e^{-\delta} \quad (\delta \gg 1 \text{ or } x_c \ll 1). \tag{40}$$

Numerical cases will be examined in Sec. V of this paper, in which the x_c parameter will be obtained from Eq. (36) along with the following expression of the Thomas-Fermi wave vector[21]

$$k_c^2=6\pi m_0 e^2/E_F=2.4435/r_s \text{ (a.u.)}. \tag{41}$$

IV. DIPOLE TRANSITIONS

It is difficult to make an *a priori* estimate of the relative importance of the two coupling terms in the full Hamiltonian (11) for effecting raising dipole transitions of the electron on the scattered ion. Two processes are to be expected: (i) direct excitation by the last term, i.e., dipole-dipole scattering, and (ii) indirect dipole excitation by the monopole (dynamical) image charge. We want to evaluate both processes, as well as possible interferences between them, by exploiting our knowledge of the exact wave function of the reduced Hamiltonian (19).

From (20) the exact evolution operator of the unperturbed system described by $H_{\text{red}}+H_e$ is

$$U_0(t)=e^{-i(H_e+H_p)t}\mathfrak{D}(t). \tag{42}$$

Then, according to formal scattering theory,[22] the evolution operator of the full Hamiltonian $H=H_{\text{red}}+H_e+H_{ep}$ is

$$U(t)=U_0(t)T\exp\left[-i\int_{-\infty}^{t} dt' H_{ep}^I(t')\right], \tag{43}$$

where T is the chronological-ordering operator and where $H_{ep}^I(t)$ is the interaction representation of H_{ep}, namely

$$H_{ep}^I(t)=U_0^{\dagger}(t)H_{ep}(t)U_0(t). \tag{44}$$

In this paper we shall consider only processes of first order in H_{ep} which are governed by

$$U(t)=U_0(t)\left[1-i\int_{-\infty}^{t} dt' U_0^{\dagger}(t')H_{ep}(t')U_0(t')\right]. \tag{45}$$

The perturbation term is obtained with standard canonical transformation formulas:

$$U_0^{\dagger}H_{ep}U_0=A\int d\vec{k}\sum_i [\lambda_{ki}(a_k+I_k^*)e^{-i\omega_k t}+\lambda_{ki}^*(a_k^{\dagger}+I_k)e^{i\omega_k t}](c_0^{\dagger}c_i e^{-i\omega_0 t}+c_i^{\dagger}c_0 e^{i\omega_0 t}), \tag{46}$$

where $\omega_0=E_1-E_0$ is the transition energy, and where we have made use of the property (22).

To shorten the notation, let us introduce the c number

$$F_i(t)=iA\int d\vec{k}\int_{-\infty}^{t}[\lambda_{ki}(\tau)I_k^*(\tau)e^{-i\omega_s t}+\text{cc}]\,d\tau \tag{47}$$

and the field operator

$$\hat{G}_i(t)=iA\int d\vec{k}\int_{-\infty}^{t} d\tau\,\lambda_{ki}^*(\tau)a_k^{\dagger}e^{i(\omega_s+\omega_0)\tau}. \tag{48}$$

Assuming that at time $t=-\infty$ the system is in the ground state $|\{0_k\},0\rangle$ of $H_{\text{red}}+H_e$, the wave function to

first order in H_{ep} is then

$$|\Psi(t)\rangle = U(t)\,|\{0_k\}, 0\rangle = e^{-i(H_e+H_p)t}\mathfrak{D}(t)\left\{|\{0_k\}, 0\rangle - \sum_i [F_i(t)+\hat{G}_i(t)]\,|\{0_k\}, i\rangle\right\}. \tag{49}$$

The first term describes the ion scattering without dipole excitation as studied in the previous section and the second term corresponds to states in which the P states $|i\rangle$ have been populated at the same time as plasmons are excited by $\hat{G}_i$ and displaced by $\mathfrak{D}$. The probability amplitude of finding at $t=\infty$ the plasmons in a final energy state $|\{n_f\}\rangle$, energy E_f, *and* the electron in excited state $|i\rangle$ is $\langle\Psi(t)\,|\{n_f\}, i\rangle$. Therefore the probability $P_i(\omega)$ for the ion to get excited and lose energy ω is

$$P_i(\omega) = \sum |\langle\Psi(\infty)\,|\{n_f\}, i\rangle|^2 \delta[\omega - (E_f + E_1 - E_0)]\,. \tag{50}$$

Completeness of the $|\{n_f\}\rangle$ states is exploited in the usual way by introducing the Fourier transform

$$P_i(\omega) = \frac{1}{2\pi}\int_{-\infty}^{+\infty} dt\, P_i(t) e^{i(\omega-\omega_0)t} \tag{51}$$

with the result for the correlation function

$$P_i(t) = \langle\Psi_i(\infty)\,|e^{-iH_p t}\,|\Psi_i(\infty)\rangle\,, \tag{52}$$

where, apart from irrelevant phase factors,

$$|\Psi_i(\infty)\rangle = \langle i\,|\Psi(\infty)\rangle = \mathfrak{D}[F_i(\infty)+\hat{G}_i(\infty)]\,|\{0_k\}\rangle. \tag{53}$$

After some operator manipulations, the correlation function (52) is found to be

$$P_i(t) = \langle 0\,|(F_i^* + \hat{G}_i^\dagger)\mathfrak{D}^\dagger e^{-iH_p t}\mathfrak{D}(F_i+\hat{G}_i)\,|0\rangle\,, \tag{54}$$

$$P_i(t) = P_0(t)\{[F_i + G_i(e^{-i\omega_s t}-1)] \times [F_i^* + G_i^*(e^{-i\omega_s t}-1)] + D_i e^{i\omega_s t}\}, \tag{55}$$

where $P_0(t)$ is the zero-excitation correlation function obtained in (26) and where

$$G_i = iA\int d\vec{k}\int_{-\infty}^{+\infty} d\tau\, \lambda_{ki}^*(\tau) I_k(\tau) e^{i(\omega_s+\omega_0)\tau}\,, \tag{56}$$

$$D_i = \left|A\int d\vec{k}\int_{-\infty}^{+\infty} d\tau\, \lambda_{ki}^*(\tau) e^{i(\omega_s+\omega_0)\tau}\right|^2. \tag{57}$$

G_i^* is the eigenvalue of the operator $\hat{G}_i^\dagger$ for the coherent amplitude eigenstate $\mathfrak{D}|\{0_k\}\rangle$.

The excitation-loss spectrum $P_i(t)$ is therefore a convolution of the no-excitation loss spectrum $P_0(t)$, with additional loss and excitation factors dependent on the dipole transition matrix elements Q_i. Whereas it does not appear possible to disentangle these interfering processes in the excited-ion spectrum, the average of the excitation-loss spectrum

$$P_i = \int_{-\infty}^{+\infty} d\omega\, P_i(\omega) = \int_{-\infty}^{+\infty} dt\, P_i(t)\delta(t) \tag{58}$$

is seen, from (55), to separate into additive terms:

$$P_i = |F_i|^2 + D_i\,. \tag{59}$$

P_i gives the overall $|0\rangle \to |i\rangle$ excitation probability irrespective of the plasmon state left behind. From the structure of F_i in (47), one recognizes the significance of the first term in (59): The ion monopole "prepares" the plasmon field into the coherent state $|\{I_k^*\}\rangle$, which includes the ion-plasmon coupling to all orders; the plasmons, in turn, induce first-order dipole transitions through the electron-plasmon coupling λ_{ki}.

On the other hand, the second additive term D_i accounts for first-order excitation processes from the direct coupling between electron and plasmons. As seen from (57), this term is the only one to survive when the monopole-plasmon interaction is turned off ($\gamma_k = 0$). This means that fast, polarizable neutral atoms or molecules scattering off metal surfaces at grazing incidence are also liable to get excited and fluoresce by the image-dipole processes investigated in the present paper.

In the next section, we shall see that the D_i term in (55) and (59) often dominates the other terms F_i and G_i in the excitation process. If we neglect the latter, the loss spectrum of excited particles (51) is seen to be of identical shape to the loss spectrum of unexcited particles, but its position relative to the elastic peak is shifted further downward by an amount $\hbar(\omega_0+\omega_s)$.

V. APPLICATIONS

In this section, we apply the theory to practical cases which could be investigated experimentally in view of testing the validity of the scattering mechanism proposed here.

A. Loss spectra

1. Large-x_c case

Consider a fast ion beam with forward velocity $v_\parallel = 5\times10^8$ cm/sec (0.15 MeV H_2^+ or 0.5 MeV He^+) impinging at grazing angle $\Phi = 0.5^\circ$ on an Al surface ($r_s \simeq 2$, $\omega_s \simeq 1.8\times10^{16}$ sec^{-1}). From (41) the cutoff wave vector k_c is $k_c \simeq 2$ Å^{-1}. This gives $x_c \simeq 6$ for which we may use the large x_c limit (37) of Eq. (33). The strength of the Poisson distribu-

tion (which gives also the average energy loss) is

$$Q=\frac{\pi}{137}\frac{c}{v_{\parallel}}\frac{1}{\Phi}\simeq 160.$$

Hence, the loss spectrum should have a nearly Gaussian shape with peak at $Q\hbar\omega_s = 1.75$ keV below the elastic energy and with a full width at the half maximum (FWHM) of order $2(2\ln 2)^{1/2}\sqrt{Q\hbar\omega_s}$ $\simeq 330$ eV. The H_2^+ beam loses 1.2% of its kinetic energy by a single surface scattering.

If a beam of α particles ($z=2$) were used instead of He^+ in the same conditions, the strength would be $Q\simeq 640$. This is a very efficient way of producing an abundant number of surface plasmons.

2. *Small-x_c case*

If one works with $v_{\parallel}=0.5\times 10^8$ cm/sec (2.5 keV H_2^+ or 5 keV He^+) in the same geometrical conditions as above, one has $x_c\simeq 0.57$, and, by using tables of Ref. 30 to evaluate (38), one finds $I(\delta\simeq 3.5)\simeq 0.0173$ and

$$Q=\frac{2}{137}\frac{c}{v_{\parallel}\Phi}I\simeq 17.5.$$

The spectrum is again of asymmetrical Gaussian shape peaking at $Q\hbar\omega_s\simeq 200$ eV below the elastic energy and with a FWHM $\simeq 110$ eV. The H_2^+ beam loses 8% of its energy on the average, and an equivalent α-particle beam would lose 16%, at which point some recoil effect should be taken into account and moderate somewhat the plasmon production.

So far there are no ion energy-loss measurements taken under conditions of small grazing angle, sufficient surfaces flatness and cleanliness, etc., appropriate for testing the effectiveness of the surface-plasmon-loss mechanism alone. The line shapes observed by Andrä *et al.*[23] and Hou *et al.*[24] are not unlike those predicted above, but the observed losses are often more important than the ones calculated on the basis of Eq. (33). For instance, Andrä *et al.*[23] obtained a peak intensity at 4 keV below the elastic energy for 153 keV N^+ ions scattering off a Cu surface at 1° grazing incidence. For such a case, Eq. (33) predicts an average loss of order 0.4 keV and a much narrower width than the observed FWHM of 6 keV.[23] Both experimental and theoretical reasons can be advanced to account for the larger losses. First, as a result of surface roughness, a substantial fraction of the incoming beam intensity must penetrate inside the bulk of the target and be subjected to large bulk losses. That the beam penetrates partly seems to be manifested by the strong dependence of the loss spectrum on spectrometer aperture.[23] An increase of the aperture around the specular direction increases the average loss and the spectral width, indicative of the fact that those ions which do penetrate scatter more diffusely, and with larger energy losses. Second, as noted in Sec. II, it is theoretically expected that the actual smooth trajectory of specularly reflected ions must yield enhanced losses as compared to those obtained with the cusp trajectory of Eq. (16). To demonstrate this effect let us reconsider the calculation of the strength Q in Eq. (33) by using the hyperbolic path (17) in which Z_1 and Z_2 are such that the distance of closest approach $Z_0=Z_1-Z_2$ is identical to that of the cusp trajectory in Eq. (16). The time integral in the amplitude (23) can be done in terms of the modified Bessel function of first-order K_1.[20] The angular integral in Eq. (26) proceeds as before with the help of Eq. (32). Using the exponential cutoff in Eq. (35), the end result for the strength (33) is now

$$Q_h=\frac{2z^2e^2}{v_{\perp}}\int_1^{\infty}dx\,\gamma^2e^{-\beta x}\frac{x}{(x^2-1)^{1/2}}K_1^2(\gamma x), \tag{60}$$

where subscript h refers to the hyperbolic path and where

$$\beta=\frac{2\omega_s}{v_{\parallel}}(k_c^{-1}-Z_2),\quad \gamma=\frac{Z_1\omega_s}{v_{\parallel}}. \tag{61}$$

This is to be compared with the cusp trajectory result Q_c given by Eqs. (33) and (38), namely

$$Q_c=\frac{2z^2e^2}{v_{\perp}}\int_{\delta}^{\infty}K_0(z)dz, \tag{62}$$

where

$$\delta=\beta+\gamma \tag{63}$$

which results from the condition of the same impact parameter Z_0. Hence one obtains an enhancement factor

$$\frac{Q_h}{Q_c}=\gamma^2\int_1^{\infty}dx\,e^{-\beta x}\frac{x}{(x^2-1)^{1/2}}K_1(\gamma x)\Big/\int_{\delta}^{\infty}dz\,K_0(z). \tag{64}$$

The actual value of this ratio is quite sensitive to the values of the parameters Z_1 and Z_2, which can only be obtained from a calculation of channeling trajectories.[10] Both parameters are of order 1 Å. In frequent practical cases, $v_{\parallel}<Z_1\omega_s\simeq 2.10^8$ cm/sec (80 keV He^+, 0.8 MeV Ar^+). Then $\gamma>1$, and, from the asymptotic expansion of modified Bessel functions,[20] $K_1^2(\gamma x)\simeq(\pi/2\gamma x)[\exp(-2\gamma x)]$. Hence

$$\lim_{\gamma\gg 1}\frac{Q_h}{Q_c}=\frac{\pi}{2}\gamma K_0(\delta)\Big/\int_{\delta}^{\infty}K_0(z)dz>\frac{\pi}{2}\gamma. \tag{65}$$

Thus for small velocities compared to $c/137$, the enhancement factor may be quite large.

For the subsequent applications of the plasmon excitation process, we have used the simpler

cusp trajectory (16) which allows analytical treatment up to the end.

B. H_2^+ dissociative scattering

We need to evaluate the quantity (59) suitably adapted for the relevant excitation of the H_2^+ ion. It is well known from molecular spectroscopy[25] that the H_2^+ ion has essentially one stable state, namely the $1s\sigma^2\Sigma_g$ ground state, and that its first electronic excited state is the unstable $2p\sigma^2\Sigma_u$ state. The $|1s\sigma_g\rangle \rightarrow |2p\sigma_u\rangle$ transition carries roughly one third of the total ground-state-dipole-oscillator strength of one. Exact oscillator strength calculations as a function of nuclei separation D have been carried out by Bates.[26] Also, the theoretical cross sections for this transition induced by charge or neutral-particle scattering,[27] as well as by optical dissociative absorption,[28] have been calculated.

In the present grazing-incidence-scattering situation, we envisage the randomly oriented molecular axis to remain fixed in space during the useful part of the beam trajectory, while the ion-surface plasmon coupling is appreciable. The spatial extent, above the metal surface, of the interaction zone is ill defined owing to the power-law behavior of the image potentials. However, if, for the sake of argument, we assume that the active zone is within 5 Å of the surface, the flight time of the ions within this distance is of order 10^{-7} cm/$\Phi v_{\parallel}$ $\simeq 2\times 10^{-14}$ sec for $v_{\parallel}\simeq 3\times 10^{8}$ cm/sec (100 keV H_2^+). This is short compared to rotational periods, but of the same order of magnitude as the H_2^+ vibrational period ($\omega_{\text{vib}}\simeq 2300$ cm^{-1}),[25] which implies that initial and final vibration states ought to be taken into consideration in this type of scattering experiment. For lower velocities, rotational degrees of freedom should also enter.

Referring to Fig. 2 where the geometry is further defined, the relevant matrix element entering the Hamiltonian (11) is now

$$\lambda_{kn}= Q_n C_k \vec{K}\cdot\vec{D}^0 e^{-kZ+i\vec{k}\cdot\vec{Y}}, \tag{66}$$

where $\vec{D}^0=\vec{D}/D$ is the molecular-axis direction, and where

$$Q_n=\int_0^\infty \langle 1s\sigma_g|\vec{r}\cdot\vec{D}^0|2p\sigma_u\rangle \Phi_n(D)\Phi_f(D)dD. \tag{67}$$

Q_n is the dipole length along the molecular direction $\vec{D}^0$ for a Franck-Condon transition occurring between the nth vibrational level $\Phi_n(D)$ of the ground state and the excited state with nuclear wave function $\Phi_f(D)$ [Fig. 2(b)]. If we assume, as is often done,[28] that the final wave function Φ_f is a suitably normalized δ function at the classical turning point D_c [Fig. 2(b)], Q_n reduces to

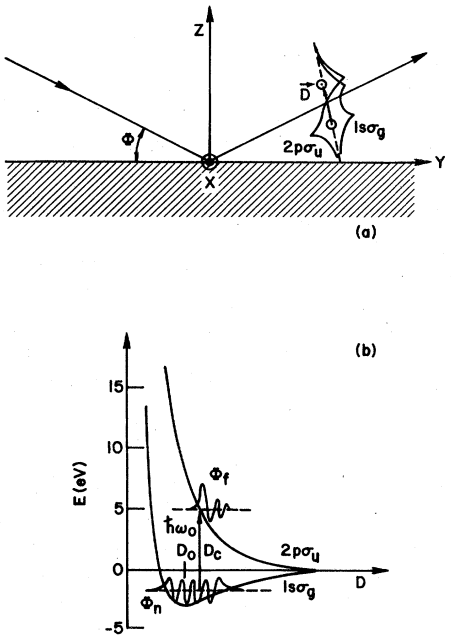

FIG. 2. (a) Schematization of the specular scattering of H_2^+ with fixed molecular axis $\vec{D}$. The interaction with surface plasmons induces strong dipole transitions between the electron states indicated in (b) where Φ_n is the nth vibrational level of the ground state $1s\sigma_g$, and Φ_f, the dissociative $2p\sigma_u$ state.

$$Q_n(D_c)= Q(D_c)\Phi_n(D_c), \tag{68}$$

where $Q(D_c)$ is the dipole length for separation D_c, as listed by Bates.[26] $\Phi_n(D_c)$ is simply the probability amplitude for finding the internuclear distance at value D_c when the raising transition occurs. If p_n is the relative incident beam intensity in vibrational state Φ_n, as determined by the more-or-less known[29] beam preparation process, the dissociation probability after scattering should be calculated as an average over the 19 or so vibrational levels of H_2^+.

$$P=\sum_{n=0}^{18} p_n \int d\vec{D}_c Q_n^2(D_c) P_n(\vec{D}_c), \tag{69}$$

where $P_n(\vec{D}_c)$ is the excitation probability which we are able to obtain from the general result (59).

Rather than carrying out the full calculation sketched above, we will satisfy ourselves, in the present feasibility evaluation, with obtaining only the dissociation probability for $\vec{D}$ perpendicular to the surface, for D_c equal to the equilibrium proton separation $D_0=1.06$ Å, and for the ground-state vibrational level Φ_0. The corresponding Franck-Condon energy is $\hbar\omega_0\simeq 10$ eV. The dipole length is obtained from Bates' table[23] of oscillator strengths f:

$$Q_0^2(1.06\text{Å}) = \frac{3}{2m\omega_0} f \simeq (1\text{Å})^2 . \tag{70}$$

To evaluate (59), the time integrals appearing in (47) and (57) are easily evaluated using the time-dependent $I_k(\tau)$ of Eq. (27) and $\lambda_k(\tau)$ of (60). The results are

$$F = \frac{z^2e^2\omega_s}{4\pi} Q_0 \int d\vec{k} S^2(k) \{4\,\mathrm{Re}[(\Omega_k + ikv_\perp)^{-1}(i\omega_0 - 2kv_\perp)^{-1}] + 2\,\mathrm{Im}(\Omega_k + ikv_\perp)^{-1}[(\omega_0 - \Omega_k + ikv_\perp)^{-1} - (\omega_0 + \Omega_k + ikv_\perp)^{-1}]\}, \tag{71}$$

$$D = \frac{z^2e^2\omega_s}{\pi} Q_0^2 \int d\vec{k} kS^2(k)[\mathrm{Im}(\omega_0 + \Omega_k - ikv_\perp)^{-1}]^2 . \tag{72}$$

These formulas are valid for general incidence, but one must keep in mind that the specular, non-penetrating reflection trajectory used to derive them applies only at grazing incidence. Using the grazing-angle condition (31), it is seen that the second term in F drops out except for a weak resonance at $\omega_0 = \Omega_k$. One obtains

$$F = \frac{z^2e^2\omega_s}{4\pi} Q_0 \int d\vec{k} S^2(k) \times \left(\frac{4\pi}{\omega_0}\delta(\Omega_k) + 2\pi i \frac{kv_\perp}{\omega_0^2}\delta(\omega_0 - \Omega_k)\right), \tag{73}$$

$$D = \frac{z^2e^2\omega_s}{\pi} Q_0^2 \int d\vec{k} kS^2(k) \frac{\pi}{kv_\perp}\delta(\omega_0 + \Omega_k) . \tag{74}$$

For $v_\perp$ sufficiently small, the second term in F may be left out. The angular integrals are done by means of (32):

$$F = \frac{2z^2e^2k_c^2}{\omega_0} Q_0 \frac{1}{x_c^2} \int_1^\infty dx \frac{xS^2(x)}{(x^2-1)^{1/2}} , \quad x_c = k_c v_\parallel/\omega_0 , \tag{75}$$

$$D = \frac{2z^2e^2}{v_\perp}(k_cQ_0)^2 \frac{\omega_0 + \omega_s}{\omega_0} \frac{1}{y_c^2} \int_1^\infty dy \frac{yS^2(y)}{(y^2-1)^{1/2}} \left(y_c = \frac{k_c v_\parallel}{\omega_0 + \omega_s}\right). \tag{76}$$

Thus the direct dipole-dipole term D which involves the "fine-structure constant" $e^2/v_\perp$ is likely to dominate the dissociative excitation process at most velocities.

The final x and y integrals will be evaluated with the exponential cutoff function $S(x) = \exp(-x/x_c)$. They are then the modified Bessel function[20] $K_1(2/x_c)$, defined and tabulated in Ref. 32. Limiting expressions are

$$K_1\left(\frac{2}{x_c}\right) = \begin{cases} \frac{1}{2}x_c \text{ for } x_c \gg 1 , \\ \left(\frac{\pi x_c}{4}\right)^{1/2} e^{-2/x_c} \text{ for } x_c \ll 1 . \end{cases} \tag{77}$$

Introducing the parameters used before ($v_\parallel \simeq 5\times10^8$ cm/sec, $\Phi = 0.5°$, $\omega_s = 11$ eV, and $\omega_0 = 10$ eV) into (69) and (70), one finds $F^2 \simeq 4$ and $D \simeq 120$. Such larger-than-one "probabilities" simply mean complete breakdown of first-order perturbation theory to calculate dissociation rates in such conditions. It also means that higher-order multipole transitions of even weak oscillator strengths are likely to be induced in the scattering of ions or neutrals, as it is in fact seen experimentally, e.g., with Ar^+ ions.[7]

For convenience, the function $F(x_c) = x_c^{-2} K_1(2/x_c)$ is plotted in Fig. 3. In terms of this function, the dissociation probability of H_2^+ on Al is

$$P = F^2 + D = 40F^2\left(\frac{x_c}{2}\right) + \frac{1.2\times10^3}{\Phi v_\parallel}\frac{\omega_s + \omega_0}{\omega_s} F\left(\frac{y_c}{2}\right) \tag{78}$$

with Φ in degrees and $v_\parallel$ in 10^8 cm/sec. Thus P is an extremely sensitive function of $v_\parallel$ at smaller energies (small x_c). With the experiment of Heiland *et al.* on H_2^+ and Ni surfaces,[2] one may estimate $\omega_s \simeq 15$ eV and $v_\parallel \simeq 0.25\times10^8$ cm/sec ($E_0 = 600$ eV), $\Phi = 15°$. This gives $y_c = 0.085$, $F(y_c/2) \simeq 0.2\times10^{-3}$, and $P \simeq 3\%$. If k_c were taken to be 3 Å^{-1} or $\omega_0 \simeq 8$ eV (corresponding to excitation

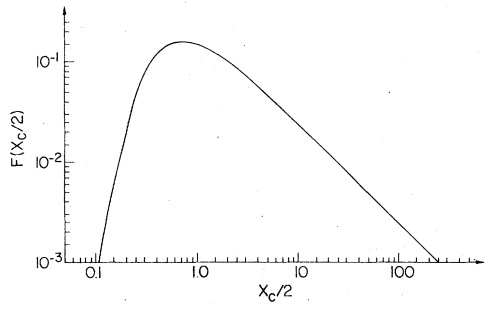

FIG. 3. Behavior of the H_2^+ dissociation probability by surface plasmons as a function of the forward beam velocity. The "probability", obtained here in first-order scattering theory, can be calculated from F by using Eq. (78) and $x_c = k_c v_\parallel/\omega_0$, $y_c = k_c v_\parallel/(\omega_0 + \omega_s)$ with k_c given by Eq. (41).

from vibrationally excited states) or $v_{\parallel} \simeq 0.35 \times 10^8$ cm/sec ($E_0 = 1200$ eV), the probability value P would be boosted above 1 in any one of these cases. In view of the uncertainty on the k_c and ω_0 parameters, we cannot quantitatively assert the degree of agreement of the present theory with the observed spectra without a full calculation along the lines indicated in (69) above and with a specular trajectory of the smooth kind as in (17). Grazing angles smaller than 15° are also required for the specular scattering condition to hold. However, the present evaluation suggests that the H_2^+ survival fraction should drop drastically when the forward kinetic energy changes from, say, 200 eV to 2 keV as in fact is seen by Heiland *et al.*[2] on going from 600 eV to 1200 eV H_2^+ on Ni (111) or W (100).

C. Production of coherent P states

From the form of the total wave function (49), these scattered ions, which will eventually fluoresce at frequency ω_0, have been prepared by the scattering process into the coherent superposition of P states $|i\rangle$:

$$|\psi_{ex}\rangle = \sum_{i=x,y,z} \hat{G}_i |\{0_k\}\rangle\, |i\rangle \quad . \tag{79}$$

$$= i \sum_i A \int d\vec{k} \int_{-\infty}^{+\infty} d\tau\, \lambda_{ki}^*(\tau) e^{i(\omega_0+\omega_s)\tau} |\{0_l\}' 1_k\rangle\, |i\rangle\,, \tag{80}$$

where, from our experience with the previous application, we have neglected the F_i terms in (47) and where $|\{0_l\}' 1_k\rangle$ is the plasmon-field ground state except for the $\vec{k}$ wave which is excited once. The unitary operator $\exp[-i(H_e + H_p)t]\mathfrak{D}$ has been left out, as it does not affect the following argument.

The crucial observation is that, referring to Eqs. (10) and (13)–(15), there is a $\pi/2$ phase shift [see the structure of the $\vec{K}$ vector in Eq. (10)] between the amplitudes of the $|x\rangle$ and $|y\rangle$ states on the one hand, and of the $|z\rangle$ state on the other. This is the basic ingredient for production of orientation of polarization in the P states and subsequent radiative decay by emission of elliptically polarized light.

Assuming for simplicity that the light spectrometer is set in the x-viewing direction (Fig. 1), it is clear that the amount of elliptical polarization of the light emitted in this direction should be proportional to the average electron angular momentum J_x in the coherent state $|\psi_{ex}\rangle$. The relevant quantity here is the so-called atomic orientation or Stokes parameter[30,31]

$$\frac{S}{I} = \frac{\langle \psi_{ex} | J_x | \psi_{ex} \rangle}{\langle \psi_{ex} | J^2 | \psi_{ex} \rangle} = \left(\sum_{m=-1,0+1} m\sigma_m \right) \Big/ l(l+1) \sum_m \sigma_m \tag{81}$$

or

$$\frac{S}{I} = \tfrac{1}{2}(\sigma_+ - \sigma_-)/(\sigma_+ + \sigma_- + \sigma_0)\,, \tag{82}$$

where σ_m is the production cross section for the J_x angular momentum eigenstate $|m\rangle$. To evaluate S/I, we must rewrite the final state $|\psi_{ex}\rangle$ as a superposition of $|m\rangle$ states, which is readily done by means of the substitutions

$$|x\rangle = |0\rangle, \quad |y\rangle = \frac{1}{\sqrt{2}}(|+\rangle + |-\rangle)\,, \qquad |z\rangle = \frac{1}{\sqrt{2}i}(|+\rangle - |-\rangle)\,. \tag{83}$$

One finds

$$|\psi_{ex}\rangle = A \int d\vec{k} \int_{-\infty}^{+\infty} d\tau\, \lambda_{k\varepsilon}^* e^{i(\omega_0+\omega_s)\tau} |1_k\rangle \times (a_k |+\rangle + b_k |-\rangle + c_k |0\rangle)\,, \tag{84}$$

where

$$a_k = \frac{1}{\sqrt{2}}\left(\frac{k_y}{k} + 1\right), \quad b_k = \frac{1}{\sqrt{2}}\left(\frac{k_y}{k} - 1\right), \qquad c_k = \frac{k_x}{k}\,. \tag{85}$$

The production cross sections σ_m are the square norms of the coefficients of $|m\rangle$ in (84). Hence, using $\langle 1_k | 1_l \rangle = A^{-1}\delta(\vec{k} - \vec{l})$, one finds

$$\sigma_0 = A \int d\vec{k}\, \frac{k_x^2}{k^2} \left| \int d\tau \lambda_{k\varepsilon}^*(\tau) e^{i(\omega_0+\omega_s)\tau} \right|^2, \tag{86}$$

$$\sigma_+ - \sigma_- = A \int d\vec{k}\, 2\frac{k_y}{k} \left| \int d\tau\, \lambda_{k\varepsilon}^*(\tau) e^{i(\omega_0+\omega_s)\tau} \right|^2, \tag{87}$$

$$\sigma_+ + \sigma_- + \sigma_0 = A \int d\vec{k}\, 2 \left| \int d\tau\, \lambda_{k\varepsilon}^*(\tau) e^{i(\omega_0+\omega_s)\tau} \right|^2 = 2D_\varepsilon\,, \tag{88}$$

with D_ε as in (57). With the help of the grazing condition (31), the time and $\vec{k}$ integrals proceed without difficulty, and the final result is

$$\frac{S}{I} = \frac{[\int_1^\infty dx\, S^2(x)/(x^2-1)^{1/2} dx]}{[2\int_1^\infty dx\, x S^2(x)/(x^2-1)^{1/2}]}\,. \tag{89}$$

Using our exponential cutoff function $S^2(x)$, this is written as

$$\frac{S}{I} = \frac{1}{2}\frac{K_0(2/x_c)}{K_1(2/x_c)}\,, \tag{90}$$

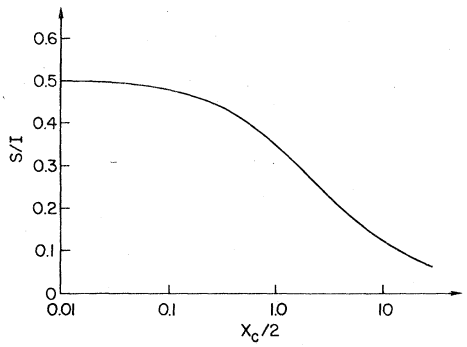

FIG. 4. Behavior of the Stokes parameter S/I defined in Eq. (90) as a function of the same parameter x_c as in Fig. 3.

where K_0 and K_1 are again modified Bessel functions tabulated in Ref. (32).

For convenience this function of $x_c = k_c v_{\parallel}/(\omega_0 + \omega_s)$ is plotted in Fig. 4. It is seen that substantial ellipticity is achieved for all interesting values of the parameters, as observed experimentally.[4,6,7] Other Stokes parameters[31] can easily be obtained in a similar manner from the wave function $|\psi_{ex}\rangle$.

VI. CONCLUSIONS

In this paper we have proposed and worked out a detailed mechanism by which surface plasmons of a metal target and individual electron transitions of a fast ion (or neutral) projectile mutually excite each other by drawing energy out of the ion kinetic energy. The simple model Hamiltonian used to describe these processes is adequate only if one can neglect ion penetration of the target, thus avoiding all bulk processes. For fast ions, this requires grazing incidence (i.e., surface channeling). The numerical examples treated indicate that the proposed mechanism is very efficient for multiple plasmon creation, dissociative excitation of molecular ions, and production of coherent atomic excited states. This calls for a treatment of the atomic multipole excitation going beyond the first Born approximation used in this work.

The grazing-incidence condition may be relaxed if one works at much lower ion kinetic energy. The model Hamiltonian, with minor modifications, is then suitable for the calculation of simultaneous excitations of target surface phonons and projectile molecular vibrations, again leading to dissociation and/or infrared polarized fluorescence.

The plasmon mechanism of coherent atomic excitation proposed here also has application to the beam-foil experiment, where thin film plasmon excitations (see Ref. 8) compete with other electronic and nuclear inelastic scattering processes.

The role of charge-transfer processes in the formation of the energy-loss spectrum can also be investigated on the basis of the model Hamiltonian of the present paper simply by considering the ion charge z as a time-dependent parameter. However, the anisotropy of the electron pickup mechanism such as studied recently by Schröder and Kupfer[33] and by Tolk *et al.*[34] is beyond the scope of the present model.

The predicted relevance of the surface-plasmon mechanism could be tested best by experimenting with structureless projectiles such as H^+ and α-particles and with metals such as Al, Mg, and Ag, which feature well-defined collective excitations. With energy resolution better than, say, 5 eV, oscillatory-ion energy-loss spectra similar to those observed in electron scattering[35] should be obtained, which would unambiguously identify multiple surface plasmon excitations as one major source of energy loss and, as a consequence, of the other inelastic effects discussed in this work.

A preliminary report of the present work has appeared in Ref. 36.

ACKNOWLEDGMENTS

This work has been performed under the auspices of the IRIS project (Institute for Research in Interface Sciences) sponsored by the Belgian Ministry for Science Policy. The author is grateful to IBM Thomas J. Watson Research Center and to IBM Belgium for a Visiting Scientist appointment. He also acknowledges the generous support from the Belgian FNRS and the Facultés N.D. de la Paix, Namur, Belgium. He has benefitted from useful conversations with Dr. J. Biersack on part of this paper and thanks the authors of Ref. 2 for sending a copy of their work in advance of publication.

*Permanet address: Facultés Notre-Dame de la Paix, B-5000 Namur, Belgium.

[1] *Inelastic Ion-Surface Collisions*, edited by N. H. Tolk, J. C. Tully, W. Heiland, and C. W. White (Academic, New York, 1977).

[2] W. Heiland, V. Beitat, and E. Taglauer, Phys. Rev. B 19, 1677 (1979).

[3] Y. B. Band, Phys. Rev. Lett. 35, 1271 (1975).

[4] T. G. Eck, Phys. Rev. Lett. 33, 1055 (1974); H. G. Berry, G. Gabrielse, and A. E. Livingston, Phys. Rev. A 16, 1915 (1977).

[5] E. L. Lewis and J. D. Silver, J. Phys. B 8, 2697

(1975).
[6]H. J. Andrä and J. D. Silver, Phys. Rev. Lett. 37, 1212 (1976).
[7]H. J. Andrä, R. Fröhling, and H. J. Plöhn, in Ref. 1, p. 329.
[8]This is similar to the case of electron-surface scattering. See, e.g., A. A. Lucas and M. Sunjić, Phys. Rev. Lett. 26, 229 (1971); Surf. Sci. 32, 439 (1972) and references therein.
[9]This paper will treat explicitly only allowed dipolar excitations.
[10]G. Varelas and J. Biersak, Nucl. Instrum. Methods 79, 213 (1970); G. Varelas and R. Sizmann, Radiat. Eff. 16, 211 (1972).
[11]R. H. Ritchie, Phys. Lett. A 38, 189 (1972); G. D. Mahan, Phys. Rev. B 5, 739 (1972).
[12]M. Schmeits and A. A. Lucas, Surf. Sci. 64, 176 (1977).
[13]A. A. Lucas, Phys. Rev. B 4, 2939 (1971).
[14]D. Langreth, in *Nobel Symposia, Medicine and Natural Sciences* (Academic, New York, 1963), Vol. 24.
[15]G. D. Mahan, in *Collective Properties of Physical Systems*, edited by B. Lundqvist and S. Lundqvist (Academic, New York, 1973).
[16]R. Glauber, Phys. Rev. 131, 2766 (1963).
[17]D. Newns, J. Chem. Phys. 50, 4572 (1969).
[18]J. Heinrichs, Phys. Rev. B 8, 1346 (1973).
[19]R. Gomer and L. W. Swanson, J. Chem. Phys. 38, 1613 (1963).
[20]I. S. Gradshteyn and I. M. Ryzhik, *Tables of Integrals, Series and Products* (Academic, New York, 1965).
[21]D. Pines, *Elementary Excitations in Solids* (Benjamin, 1965).
[22]A. Messiah, *Quantum Mechanics* (North-Holland, Amsterdam, 1963), Vol. II.
[23]H. J. Andrä and H. Winter, Hyperfine Interactions 5, 403 (1978).
[24]M. Hou, W. Eckstein, and H. Verbeek, Radiat. Eff. 39, 107 (1978).
[25]G. Herzberg, *Spectra of Diatomic Molecules* (Van Nostrand, New York, 1950).
[26]D. R. Bates, J. Chem. Phys. 19, 1122 (1951).
[27]J. M. Peek, Phys. Rev. 140, A11 (1965).
[28]G. H. Dunn, Phys. Rev. 172, 171 (1968).
[29]G. H. Dunn, J. Chem. Phys. 44, 2592 (1966).
[30]Y. B. Band, Phys. Rev. 13, 2061 (1976).
[31]H. G. Berry, L. J. Curtis, D. G. Ellis, and R. M. Schectman, Phys. Rev. Lett. 32, 751 (1974).
[32]*Handbook of Mathematical Functions*, edited by M. Abramowitz and I. A. Stegun, NBS Applied Math. Series 55 (G. P. O., Washington, D. C., 1964).
[33]H. Schröder and E. Kupfer, Z. Phys. A 239, 13 (1976).
[34]N. H. Tolk, J. C. Tully, J. S. Kraus, W. Heiland, and S. H. Neff, Phys. Rev. Lett. 41, 643 (1978); 42, 1475 (1978).
[35]C. J. Powell, Phys. Rev. 175, 972 (1968).
[36]A. A. Lucas, Phys. Rev. Lett. 43, 1350 (1979).